

pubs.acs.org/acsaelm Article

Large Crystal Growth and THz Generation Properties of 2-Amino-5-Nitrotoluene (MNA)

Bruce Wayne H. Palmer,[†] Claire Rader,[†] Enoch Sin-Hang Ho,[†] Zachary B. Zaccardi, Daisy J. Ludlow, Natalie K. Green, Matthew J. Lutz, Aldair Alejandro, Megan F. Nielson, Gabriel A. Valdivia-Berroeta, Caitlin C. Chartrand, Kayla M. Holland, Stacey J. Smith, Jeremy A. Johnson,* and David J. Michaelis*



Cite This: https://doi.org/10.1021/acsaelm.2c00592



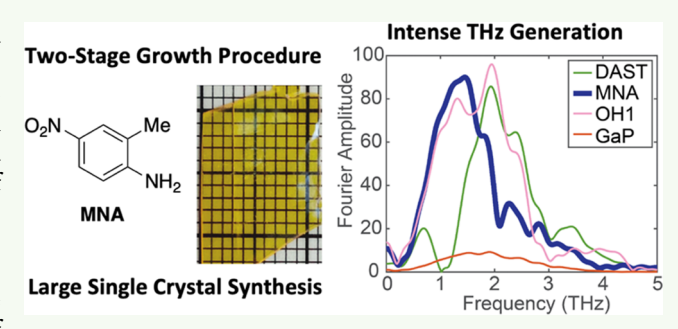
ACCESS

Metrics & More

Article Recommendations

Supporting Information

ABSTRACT: Despite being identified 4 decades ago as a potentially powerful organic material for intense terahertz (THz) generation, 2-amino-5-nitrotoluene (MNA) has not been extensively used as a THz source because of challenges associated with synthesizing large single crystals of the material. We report a consistent two-step process for growing large single crystals of MNA that are suitable for high intensity terahertz (THz) generation via optical rectification of IR light. Our process includes initial sublimation growth of thin sheets or needles of MNA, followed by solution phase slow evaporation growth using the sublimated crystals as seeds. To demonstrate the usefulness of



MNA as a nonlinear optical crystal, we characterize the THz generation properties of MNA and compare these results to state-of-the-art organic THz generators such as OH-1, 4-N,N-dimethylamino-4'-N'-methylstilbazolium 4-methylbenzenesulfonate (DAST), and N-benzyl-2-methyl-4-nitroaniline (BNA). We further determine the dependence of THz intensity on crystal thickness and pump wavelength, determine the THz efficiency at different pump powers, and report the THz refractive index and absorption coefficient. These results demonstrate that high-quality MNA crystals provide a useful source for high intensity THz generation.

KEYWORDS: terahertz generation, nonlinear optical crystal, crystal growth, X-ray crystallography, 2-amino-5-nitrotoluene

1. INTRODUCTION

2-Amino-5-nitrotoluene (MNA) was identified as early as 1981 as a potentially powerful molecular building block for nonlinear optical (NLO) applications, due to its large microscopic hyperpolarizability. The large hyperpolarizability results from highly asymmetric charge correlated excited states of the π electronic structure of the molecule. However, MNA crystal growth efforts over the past ~40 years have been unable to generate large, high-quality crystals needed for NLO applications. To circumvent these crystallization challenges, a benzyl group was added to MNA to form N-benzyl-2-methyl-4-nitroaniline (BNA) nearly 20 years after the molecular building block of MNA was introduced. This additional benzyl group enhances the crystallization properties of MNA, and made it possible to produce large single crystals of BNA. The addition of the benzyl group in BNA, however, increases the packing volume of the molecule without significantly increasing its hyperpolarizability, thus leading to lower packing density of BNA when compared to the crystal structure of MNA. The lower density of chromophores in BNA's crystal structure reduces the potential NLO efficiency.³ Even so, BNA has in recent years become a widely used NLO crystal, particularly for intense terahertz (THz) generation. 4-8 When pumped with near infrared (NIR) light, BNA produces a broad

THz spectrum with much greater efficiency than inorganic crystals like ZnTe and GaP.⁸

THz spectroscopy is a powerful tool for many sensing, imaging, and communications applications due to the unique interactions that THz radiation has with different materials. Many of the emerging applications of THz spectroscopy require the generation of intense THz pulses with a broad spectrum. Intense THz light can be efficiently generated via optical rectification in organic NLO crystals, where NIR frequency light is down-converted to THz frequencies. For efficient THz generation, organic NLO materials must have high molecular hyperpolarizability and pack in a noncentrosymmetric alignment in the crystal state. One of the most significant challenges in developing new organic THz generators is the need to grow large single crystals (>3 × 3 × 0.5 mm³) that can be irradiated for THz generation. As

Received: May 4, 2022 Accepted: August 3, 2022



described above, growing large, high-quality crystals for nonlinear optical applications has been a long-standing challenge for many potentially useful organic crystals such as MNA.

In this work, we present a two-step growth process that enables the formation of large MNA single-crystal plates (up to 20 mm \times 20 mm with 0.5 mm thickness) that are suitable for THz generation and other NLO applications. Our new method involves an initial sublimation growth procedure that forms medium sized sheets or needles of MNA that are ~0.1 mm thick. These thin single-crystal sheets or needles can then be used as seed crystals for crystal growth via a slow evaporation protocol. The large MNA crystals show THz generation properties that surpass those of its derivative BNA when pumped with 1250 nm light, and rival those of red-orange organic crystals like 4-N,N-dimethylamino-4'-N'-methylstilbazolium 4-methylbenzenesulfonate (DAST) and OH-1, making it one of the most efficient yellow THz generators to date. The higher molecular density of MNA in the crystalline state helps explain the improved THz generation capabilities when compared to BNA.

2. EXPERIMENTAL SECTION

2.1. Single-Crystalline Thin Sheet Growth. Previously, Damman and co-workers developed a method for growing thin sheets of MNA fused to glass substrates. In their report, they showed that these films were active for second harmonic generation. Growth of larger crystals of MNA has once been mentioned in the literature, but no detailed methods for crystal growth were described and there are no additional reports of the use of large MNA crystals. Our early attempts to grow large crystals of MNA via slow evaporation methods failed to give any suitable single crystals. We therefore turned our attention to sublimation techniques, which we believed could provide single crystalline materials for THz generation studies and for use as seeds for large crystals growth. 11

Figure 1 shows the sublimation setup and as-grown MNA sheets. In our experimental setup (Figure 1a), sublimation and crystal growth

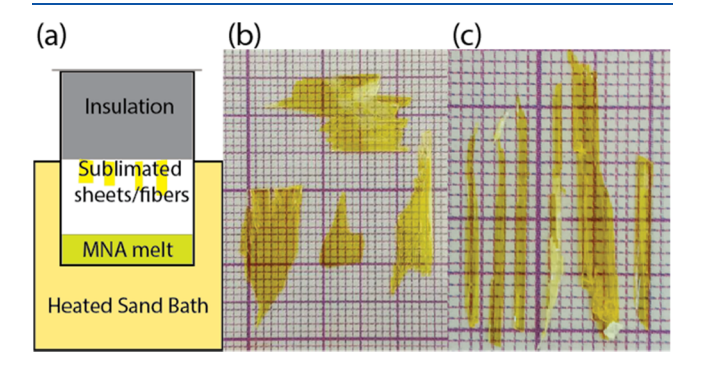


Figure 1. (a) Sublimation setup for single crystal growth. (b) Thin single crystal sheets and (c) needles of MNA grown via sublimation. Small grid squares are $\sim 1 \times 1 \text{ mm}^2$.

occurred by heating 7 g of MNA (obtained commercially from Combi-Blocks Inc.) in a 400 mL beaker to 136.6 °C for 16 h, followed by crystal growth at 129.6 °C for 7 h. The single crystals grown via sublimation were of two forms — thin sheets and thin needles (see Figure 1b,c). Following this technique, we regularly obtained MNA sheets with 3 mm \times 3 mm to 5 mm \times 5 mm in size with thicknesses of 70–150 μ m. Thin MNA sheets can be used directly for broadband THz generation, but thicker crystals (in the range of 300–600 μ m) are required for higher-power THz generation.

2.2. Slow Evaporation Growth. To grow larger surface area and thicker MNA crystals, commercially available MNA was first purified

by being dissolved in CH_2Cl_2 and filtered through a short plug of silica gel. Removal of solvent gave MNA of sufficient purity for slow evaporation growth studies. Using the long needles that were grown via our sublimation method as seeds (see Figure 1c), larger crystals were grown over a period of several days via slow evaporation from concentrated solutions of MNA in acetone. In this manner, we routinely obtained MNA single crystals of 5 mm \times 5 mm \times 0.2 mm, or larger, in size. A large area as-grown MNA crystal is shown in Figure 2a, and a cut and polished crystal is shown in Figure 2b. A total

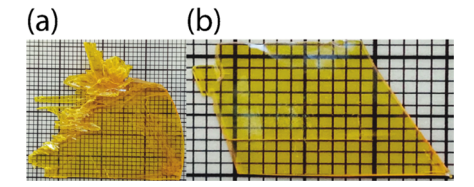


Figure 2. Large single crystals of MNA grown via slow evaporation with MNA seed crystals. (a) As grown. (b) Cut and polished.

of 33 large MNA crystals were grown to demonstrate the reproducibility of the method (see Supporting Information for crystal images). This is the first report of the growth of large single crystals of MNA suitable for intense THz generation.

2.3. X-ray Diffraction Characterization. The structure of these high-quality MNA crystals was determined by single-crystal X-ray diffraction (SC-XRD) (see Section 2 of Supporting Information for experimental details). We confirmed that our MNA crystals grew in the monoclinic crystal system in space group CC, consistent with the reported structure in the Cambridge Structural Database (CCDC ID: 643907). We also used these structures to evaluate molecular alignment within MNA. Ideal molecular alignment of an NLO crystal is head-to-tail alignment in which the molecular hyperpolarizability vectors lie in the same direction as the polar axis of the crystal. The angle, $\theta_{\rm p}$, between the polar axis and the hyperpolarizability vector is 19.5° as illustrated in Figure 3a. Using $\theta_{\rm p}$, the order parameter $(\cos^3\theta_p)$ can be calculated, with a value of 1 indicating ideal alignment. We calculated the order parameter for MNA to be 0.84, which is comparable to the value of the common NLO crystal DAST (0.83) and is higher than its derivative BNA (0.64). 12,11

An important consideration in the design of organic crystals for THz generation applications is the growth direction of the crystalline materials. To determine the indices of the largest face of the crystal, diffraction from the main face was recorded in reflection geometry and compared with the simulated MNA powder pattern (see Section 2 of Supporting Information). As Figure 3b shows, the main contributions to the pattern are from the (020) and (040) planes, which indicates that the main crystal face of MNA is (010). The molecular hyperpolarizability vectors align very well with this plane, as seen in Figure 3a. Because ideal THz generating organic crystals should have the sum of the molecular hyperpolarizability vectors oriented in plane with the irradiated crystal face, our MNA crystals grow in an ideal direction for THz generation applications.

All of our crystals were thus irradiated on the (010) face for THz generation. To determine the THz light polarization with respect to the molecular alignment, we face-indexed a strip of one of the large single crystals that had been used for THz generation as indicated in Figure 3c and described in Section 2 of Supporting Information. As Figure 3d shows, the polarization direction of the light is precisely parallel with the plane of the molecules.

3. TERAHERTZ GENERATION EXPERIMENTS

MNA crystals were characterized for THz generation using the three-parabolic mirror focusing system described in our previous work. In brief, NIR laser pulses of wavelength 1250 nm were obtained from an optical parametric amplifier that was pumped with 800-nm light from a Ti:sapphire laser system. The 1250 nm light pulse duration was \sim 100 fs with 0.7

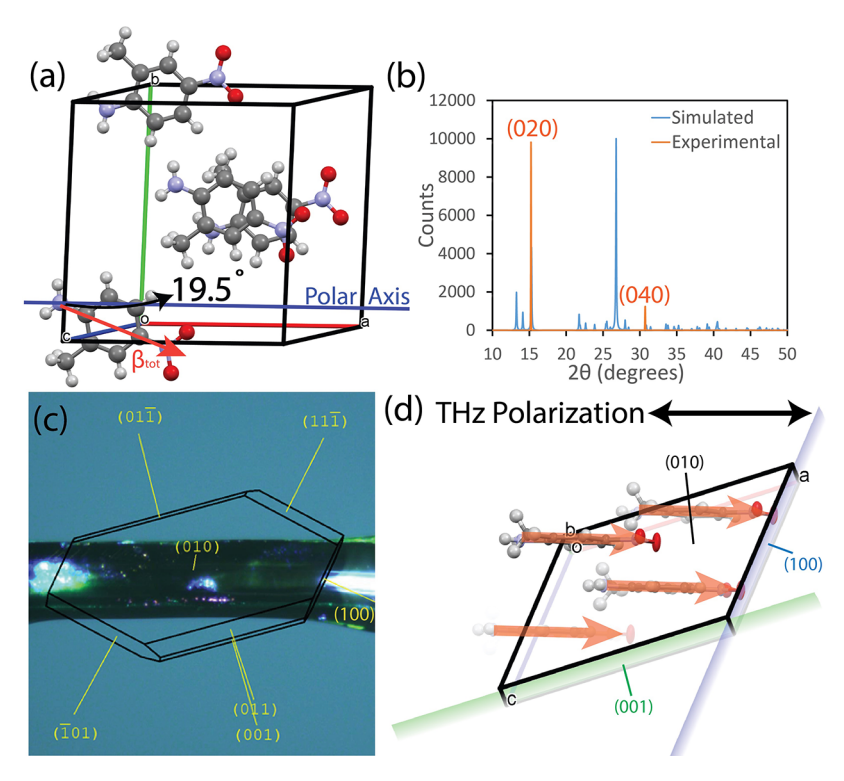


Figure 3. (a) Molecular alignment in the unit cell of MNA, showing the angle between polar axis of the crystal and hyperpolarizability vector of an MNA molecule. (b) Diffraction from the main face of MNA (orange) compared to the simulated powder pattern (blue) from CSD entry 643907. (c) Face Index of an MNA crystal strip. The crystallographic direction is indicated in yellow (d) An illustration of the 010 plane of an MNA unit cell, viewed along the *b*-axis. The hyperpolarizability vectors are indicated in orange.

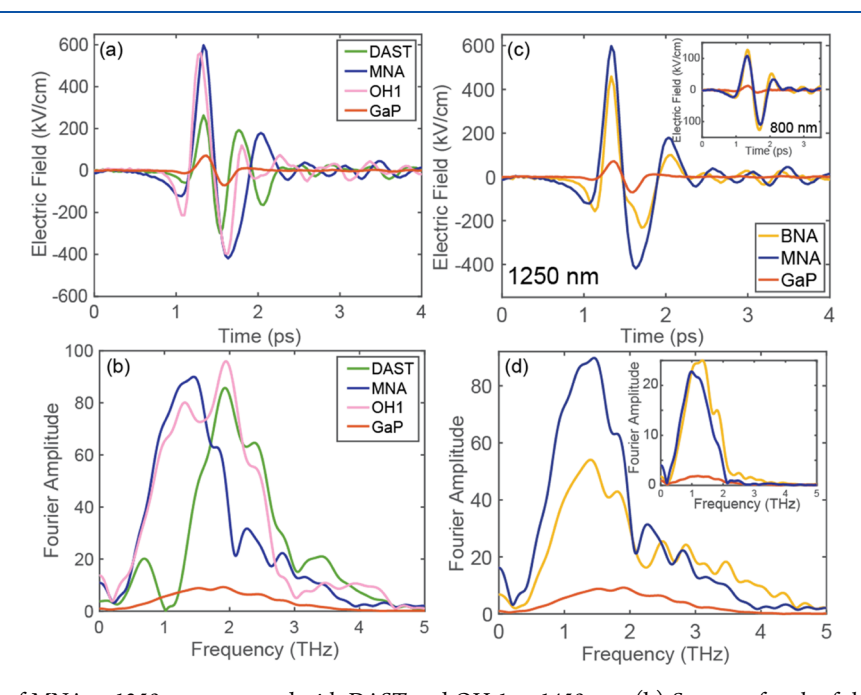


Figure 4. (a) Time traces of MNA at 1250 nm compared with DAST and OH-1 at 1450 nm. (b) Spectra of each of the crystals in (a). (c) Time traces MNA compared with GaP and BNA at 1250 nm, with an inset of the same comparison at 800 nm. (d) Spectra of each of the crystals in (c), with an 800 nm inset.

mJ per pulse and a $1/e^2$ beam diameter of ~7.6 mm. These NIR pump pulses were directed to the MNA (or other) THz generation crystal. The generated THz waves were passed through a pair wire-grid polarizers and focused using a set of three off-axis parabolic mirrors to a GaP electro-optic sampling (EOS) detection ensemble. The GaP EOS ensemble consisted

of a 100 μ m thick (110) GaP crystal fused to a 1 mm (100) GaP layer to avoid signal-echoes from the thin GaP and provide a more accurate characterization of the generated THz. A ~100 fs 800-nm probe pulse, with a variable relative delay compared to the THz pulse, was used to read out the THz electric field waveform via electro-optic sampling in the (110)

ACS Applied Electronic Materials

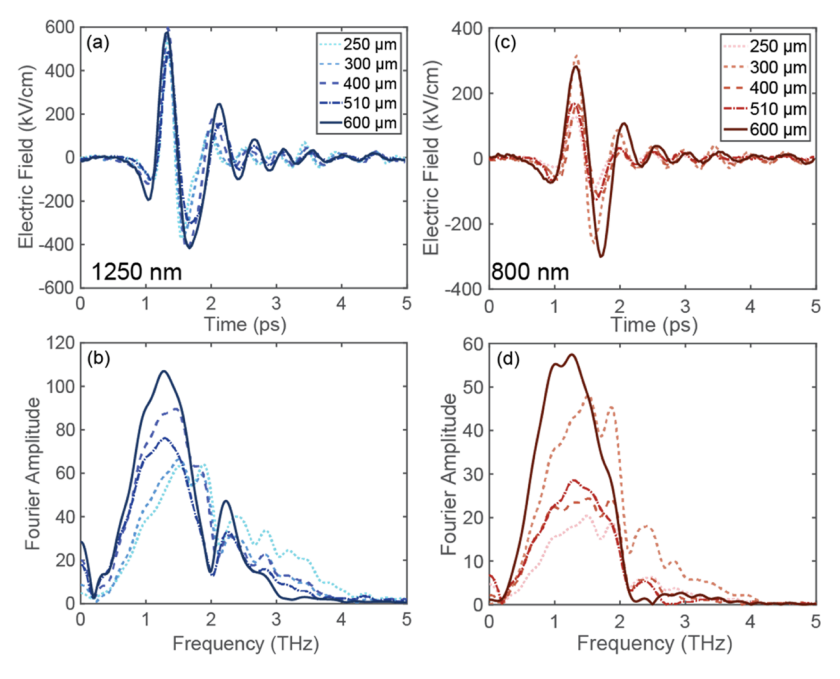


Figure 5. (a) Time traces of thick MNA crystals at 1250 nm with thicknesses ranging from 250 to 600 μ m at 1250 nm. (b) Spectra of crystals used in (a) at 1250 nm. (c) Time traces of thick MNA crystals ranging from 250 to 600 μ m at 800 nm. (d) Spectra of crystals used in (c) at 800 nm.

GaP. Due to the pulse duration, the THz detection bandwidth with this setup was restricted to ~6 THz. To compare THz generation from other NLO crystals DAST, OH-1, and GaP, we used the identical setup and nearly identical laser parameters; we kept the pump pulse energy constant but adjusted the pump wavelength to 1450 nm for both DAST and OH-1 (where they generate THz more efficiently).

THz pulses and spectra of 510 μ m thick MNA and the other NLO crystals are plotted in Figure 4. When pumped with 1250 nm light, MNA produces high field strengths on the order of 1 MV/cm (see Figure 4a,b). It has a broad, smooth spectrum, with its highest peak at 1 THz, and one main absorption dip at 2 THz, with frequency content extending out to 5 THz. With its high generated field strengths, MNA compares favorably with state-of-the-art red THz generation crystals DAST and OH-1, each with a similar thickness of \sim 400 μ m, and significantly exceeds the THz output of a 320 μ m thick GaP crystal (see Figure 4a,b). Each crystal was tested using a pump fluence of 1.32 mJ/cm². These strong THz pulses demonstrate that MNA is comparable to many state-of-the-art THz sources. It is potentially the most powerful yellow THz generator to date, making it useful in specific THz spectroscopy applications.

We also provide a direct comparison of THz generation from MNA compared to yellow BNA (which was derived from MNA). Figure 4c,d shows a direct comparison between MNA, BNA, and GaP, all pumped at 1250 nm still using a pump fluence of 1.32 mJ/cm^2 . Similar thicknesses were used for BNA and MNA ($\sim 500 \mu \text{m}$). MNA and BNA produce similar Fourier amplitudes above 2 THz, however MNA produces significantly stronger THz below 2 THz, resulting in a peak-to-peak field strength $\sim 1.6 \times$ higher than BNA. The insets to Figure 4c,d show a comparison between MNA and BNA pumped at 800 nm, with a spot size of 9 mm and a pump fluence of 1.26 mJ/cm^2 . Due to marginally better phase matching, BNA generates slightly stronger THz when pumped

with 800 nm light, with both crystals producing similar spectral content below 2 THz.

We also recorded THz generation with both 1250 and 800 nm pump wavelengths using MNA crystals with various thicknesses. The pump fluence for 1250 nm was 1.34 mJ/cm², and for 800 nm it was 2.2 mJ/cm². As shown in Figure 5a,b, good phase matching was observed at 1250 nm and all thicknesses produce intense THz pulses with fairly broad spectra. In general, thicker crystals produce larger amplitudes at lower frequencies. Figure 5c,d shows THz generation from the same crystals when pumped at 800 nm. Less optimal phase matching at THz frequencies above 2 THz results in mainly lower frequency components for crystals thicker than 300 μ m. For both pump wavelengths, the 600 μ m thick crystal produced the largest THz electric field strengths.

To better understand phase matching at longer NIR pump wavelengths, we measured THz generation of a 400 μ m thick MNA crystal from 1250 to 1550 nm and with a pump fluence of 0.66 mJ/cm². Figure 6a shows the peak field strength as a function of pump wavelength. 1250 nm enables the maximum generated field strength, and we see an initially surprising dip in generated THz at 1450 nm. This dip can be explained by the increased absorption in MNA at 1450 nm, where the green line in Figure 6a shows the transmittance of the IR pump light. Figure 6b shows generated spectra for each pump wavelength, with the inset showing normalized spectra. Our data indicate that only the spectral amplitude is significantly influenced by pump wavelength in this range.

We also measured the THz generation efficiency by measuring the THz pulse energy with a pyroelectric detector as a function of pump fluence at both 1250 and 800 nm pump wavelengths (Figure 7). At a maximum fluence of 1.3 mJ/cm², MNA produces THz with up to 3% efficiency when pumped with 1250 nm. Due to the suboptimal phase matching, the efficiency drops by an order of magnitude when pumped with 800 nm.

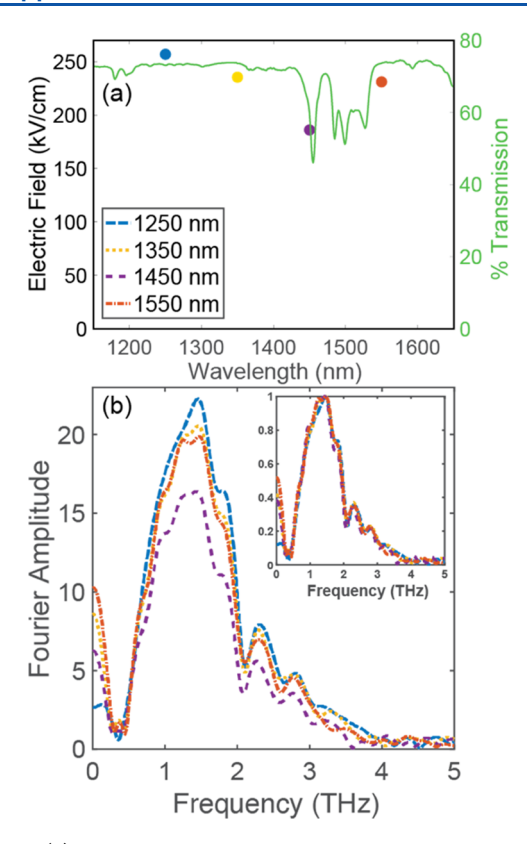


Figure 6. (a) Peak electric field strength of 400 μ m thick MNA as a function of pump wavelength 1250–1550 nm. The green line with right *y*-axis shows NIR transmission for the same wavelength range. (b) Generated spectra for each wavelength, with normalized spectra in the inset.

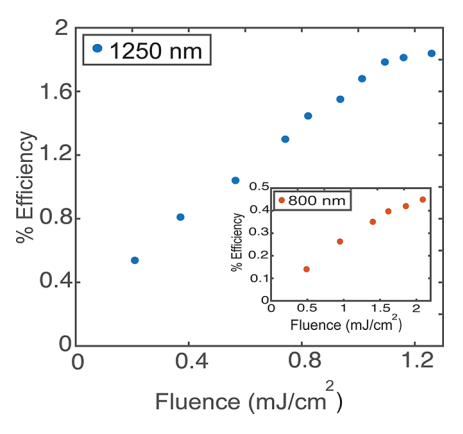


Figure 7. Percent efficiency of MNA at 1250 nm up to \sim 1.3 mJ/cm², with an inset of MNA efficiency at 800 nm up to \sim 2.0 mJ/cm².

Lastly, we performed THz transmission measurements to extract the refractive index and absorption coefficient over the range of 1–5 THz. Figure 8a,b shows the extracted refractive index and absorption coefficient of MNA (red circles), with a Lorentz oscillator fit overlaid (blue line). The refractive index and absorption coefficient of MNA show main features at 2.1, 2.7, and 4.2 THz, explaining dips in the MNA generation spectra shown in Figures 4–6 above. Over this entire frequency range, the absorption coefficient for MNA is less than 250 cm⁻¹, which contributes to the broad and smooth THz spectrum that MNA produces.

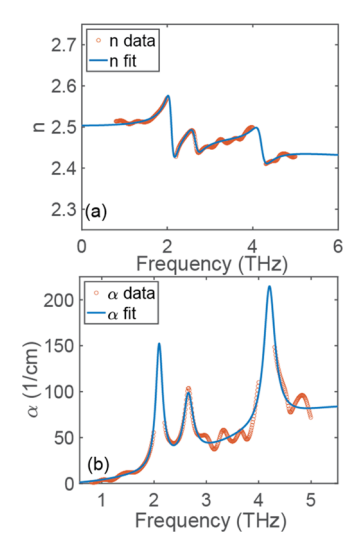


Figure 8. (a) THz refractive index and (b) absorption coefficient of MNA (red dots), with Lorentz oscillator fit (solid blue line) showing three main features at 2.1, 2.7, and 4.2 THz.

4. CONCLUSIONS

In conclusion, we have developed an effective method to consistently grow large single crystals of MNA (5 mm × 5 mm thin plates) by a two-step crystallization process. Our two-step method involves initial sublimation growth of high purity, thin needle crystals via sublimation, and these needles serve as seed crystals for slow evaporation growth in concentrated solutions of purified MNA in acetone. Our MNA crystals show THz generation efficiency that rivals and surpasses that of commonly used BNA, an MNA derivative. Our studies confirm that MNA is an excellent and readily available candidate for high intensity and broad THz generation, as MNA is commercially available and doesn't require the additional synthetic steps required for synthesizing BNA.

ASSOCIATED CONTENT

Supporting Information

The Supporting Information is available free of charge at https://pubs.acs.org/doi/10.1021/acsaelm.2c00592.

Additional experimental details and methods, including Lorentz oscillator parameters (PDF)

AUTHOR INFORMATION

Corresponding Authors

Jeremy A. Johnson — Department of Chemistry and Biochemistry, Brigham Young University, Provo, Utah 84602, United States; Email: jjohnson@chem.byu.edu

David J. Michaelis — Department of Chemistry and Biochemistry, Brigham Young University, Provo, Utah 84602, United States; orcid.org/0000-0003-3914-5752; Email: dmichaelis@chem.byu.edu

Authors

Bruce Wayne H. Palmer – Department of Chemistry and Biochemistry, Brigham Young University, Provo, Utah 84602, United States

Claire Rader – Department of Chemistry and Biochemistry, Brigham Young University, Provo, Utah 84602, United States

- Enoch Sin-Hang Ho Department of Chemistry and Biochemistry, Brigham Young University, Provo, Utah 84602, United States
- Zachary B. Zaccardi Department of Chemistry and Biochemistry, Brigham Young University, Provo, Utah 84602, United States
- Daisy J. Ludlow Department of Chemistry and Biochemistry, Brigham Young University, Provo, Utah 84602, United States
- Natalie K. Green Department of Chemistry and Biochemistry, Brigham Young University, Provo, Utah 84602, United States
- Matthew J. Lutz Department of Chemistry and Biochemistry, Brigham Young University, Provo, Utah 84602, United States
- Aldair Alejandro Department of Chemistry and Biochemistry, Brigham Young University, Provo, Utah 84602, United States
- Megan F. Nielson Department of Chemistry and Biochemistry, Brigham Young University, Provo, Utah 84602, United States
- Gabriel A. Valdivia-Berroeta Department of Chemistry and Biochemistry, Brigham Young University, Provo, Utah 84602, United States
- Caitlin C. Chartrand Department of Chemistry and Biochemistry, Brigham Young University, Provo, Utah 84602, United States
- Kayla M. Holland Department of Chemistry and Biochemistry, Brigham Young University, Provo, Utah 84602, United States
- Stacey J. Smith Department of Chemistry and Biochemistry, Brigham Young University, Provo, Utah 84602, United States

Complete contact information is available at: https://pubs.acs.org/10.1021/acsaelm.2c00592

Author Contributions

[†]B.W.H.P., C.R., and (E.)S.-H.H. contributed equally to this work.

Funding

The authors thank the National Science Foundation (DMR 2104317) for support of this research. The authors also acknowledge the Brigham Young University Simmons Research Endowment for partial funding of this work.

Notes

The authors declare the following competing financial interest(s): DJM and JAJ disclose that they are co-founders of Terahertz Innovations LLC, in which both individuals have financial interests. This work may lead to the development of products which may be licensed to Terahertz Innovations, LLC. We have disclosed those interests fully to the ACS and have in place an approved plan for managing any potential conflicts arising from this arrangement.

REFERENCES

- (1) Lipscomb, G. F.; Garito, A. F.; Narang, R. S. An exceptionally large linear electro-optic effect in the organic solid MNA. *J. Chem. Phys.* **1981**, *75*, 1509–1516.
- (2) Thirupugalmani, K.; Venkatesh, M.; Karthick, S.; Maurya, K. K.; Vijayan, N.; Chaudhary, A. K.; Brahadeeswaran, S. Influence of polar solvents on growth of potentially NLO active organic single crystals of N-benzyl-2-methyl-4-nitroaniline and their efficiency in terahertz generation. *CrystEngComm* **2017**, *19*, 2623–2631.

- (3) Kwon, O. P.; Ruiz, B.; Choubey, A.; Mutter, L.; Schneider, A.; Jazbinsek, M.; Gramlich, V.; Günter, P. Organic Nonlinear Optical Crystals Based on Configurationally Locked Polyene for Melt Growth. *Chem. Mater.* **2006**, *18*, 4049–4054.
- (4) Miyamoto, K.; Minamide, H.; Fujiwara, M.; Hashimoto, H.; Ito, H. Widely tunable terahertz-wave generation using an N-benzyl-2-methyl-4-nitroaniline crystal. *Opt. Lett.* **2008**, *33*, 252–254.
- (5) Kuroyanagi, K.; Fujiwara, M.; Hashimoto, H.; Takahashi, H.; Aoshima, S.-i.; Tsuchiya, Y. Determination of Refractive Indices and Absorption Coefficients of Highly Purified *N*-Benzyl-2-methyl-4-nitroaniline Crystal in Terahertz Frequency Regime. *Jpn. J. Appl. Phys.* **2006**, *45*, L761–L764.
- (6) Shalaby, M.; Vicario, C.; Thirupugalmani, K.; Brahadeeswaran, S.; Hauri, C. P. Intense THz source based on BNA organic crystal pumped at Ti:sapphire wavelength. *Opt. Lett.* **2016**, *41*, 1777–1780.
- (7) Miyamoto, K.; Ohno, S.; Fujiwara, M.; Minamide, H.; Hashimoto, H.; Ito, H. Optimized terahertz-wave generation using BNA-DFG. *Opt. Express* **2009**, *17*, 14832–14838.
- (8) Tangen, I. C.; Valdivia-Berroeta, G. A.; Heki, L. K.; Zaccardi, Z. B.; Jackson, E. W.; Bahr, C. B.; Ho, S.-H.; Michaelis, D. J.; Johnson, J. A. Comprehensive characterization of terahertz generation with the organic crystal BNA. *J. Opt. Soc. Am. B* **2021**, *38*, 2780–2785.
- (9) Damman, P.; Vallee, R.; Dosiere, M.; Wittmann, J. C.; Toussaere, E.; Zyss, J. Morphology and NLO properties of thin films of organic compounds obtained by epitaxial growth. *Opt. Mater.* 1998, 9, 423–429.
- (10) Wen, Z.; Grossman, C.; Garito, A.; Farhat, N. In *Total Internal Reflection Spatial Light Modulator Using Organic Electrooptic Crystal MNA*, SPIE Proceedings, 1988.
- (11) Shepherd, E. E. A.; Sherwood, J. N.; Simpson, G. S.; Yoon, C. S. The growth, perfection and properties of organic non-linear optical materials I. 4-nitro-4'-methyl benzylidene aniline. *J. Cryst. Growth* **1991**, *113*, 360–370.
- (12) Valdivia-Berroeta, G. A.; Heki, L. K.; McMurray, E. A.; Foote, L. A.; Nazari, S. H.; Serafin, L. Y.; Smith, S. J.; Michaelis, D. J.; Johnson, J. A. Alkynyl Pyridinium Crystals for Terahertz Generation. *Adv. Opt. Mater.* **2018**, *6*, No. 1800383.
- (13) Yin, J.; Li, L.; Yang, Z.; Jazbinsek, M.; Tao, X.; Günter, P.; Yang, H. A new stilbazolium salt with perfectly aligned chromophores for second-order nonlinear optics: 4-N,N-Dimethylamino-4'-N'-methyl-stilbazolium 3-carboxy-4-hydroxybenzenesulfonate. *Dyes Pigm.* **2012**, *94*, 120–126.
- (14) Zaccardi, Z. B.; Tangen, I. C.; Valdivia-Berroeta, G. A.; Bahr, C. B.; Kenney, K. C.; Rader, C.; Lutz, M. J.; Hunter, B. P.; Michaelis, D. J.; Johnson, J. A. Enabling high-power, broadband THz generation with 800-nm pump wavelength. *Opt. Express* **2021**, *29*, 38084–38094.
- (15) Scheller, M.; Jansen, C.; Koch, M. Analyzing sub-100-μm samples with transmission terahertz time domain spectroscopy. *Opt. Commun.* **2009**, 282, 1304–1306.
- (16) Kitaeva, G. Kh.Terahertz generation by means of optical lasers. *Laser Phys. Lett.* **2008**, *5*, 559–576.